TISSUE ENGINEERING: Part A
Volume 15, Number 7, 2009

DOI: 10.1089/ten.tea.2008.0227

Enhancing Osteogenic Differentiation of Mouse Embryonic Stem Cells by Nanofibers

Laura A. Smith, M.S.,[1] Xiaohua Liu, Ph.D.,[2] Jiang Hu, Ph.D.,[2]
Peng Wang, Ph.D.,[2] and Peter X. Ma, Ph.D.[1–3]

Controlled differentiation of embryonic stem cells (ESC) is necessary to their use as a cell source for tissue engineering or regeneration. To date, most studies have concentrated on chemical cues to direct ESC differentiation. However, during normal embryonic development, multiple factors beyond chemical cues play a role, including the extracellular matrix (ECM) in bone development. In this study, we use nanofibrous (NF) matrices to mimic the morphology of the ECM to examine the contribution of the ECM morphology to the differentiation of mouse ESC. After 12 h of differentiation culture, mouse ESC form protrusions interacting with NF matrices, while they appear not to interact with flat films. Immunofluorescence staining after 26 days of differentiation culture indicates a greater degree of differentiation for mouse ESC on NF matrices compared to flat films. Polymerase chain reaction results, also, show greater degree of osteogenic differentiation on NF matrices compared to flat films when osteogenic supplements are added to the culture. Overall, these results demonstrate that NF morphology contributes to the controlled differentiation of mouse ESC.

Introduction

Embryonic stem cells (ESC) typically isolated from the inner cell mass of blastocysts are pluripotent and possess the ability to differentiate into all tissues derived from the three germ layers.[1,2] Due to this, ESC hold great promise as a cell source for tissue engineering.[3] Additionally, ESC have been found to proliferate longer than other types of stem cells, making them a potentially advantageous cell source. ESC-derived cells have just begun to be explored as the cell source for tissue engineering applications.[4–7]

Much of the effort to control the differentiation of ESC into specific lineages has focused on the use of biological factors.[8–10] However, it is known that extracellular matrix (ECM) contributes to the osteogenic lineage selection during embryonic development through cytoskeletal and surface receptor interactions.[11–13] Therefore, to successfully use ESC in tissue engineering, we need to understand and mimic the contributions of the ECM. The scaffold should act as a directive template for the ESC, stimulating the desired differentiation pathway much as the ECM does during embryonic development. As such, the scaffold should mimic the natural ECM of the desired tissue.[14] Type I collagen, consisting of three collagen polypeptide chains wound together to form a ropelike superhelix that assembles into the fibers ranging in size from 50 to 500 nm,[15,16] is a major component of the ECM in many tissues.

We hypothesize that such nanofibers advantageously support ESC differentiation because they provide a microenvironment for cells more similar to the type 1 collagen ECM than traditional smooth surfaces. Synthetic three-dimensional nanofibers of the same size scale as natural type I collagen have been developed in our lab using a novel phase separation technique.[17–21] To test our hypothesis, thin poly(L-lactic acid) (PLLA) matrices with nanofibrous (NF) architecture and flat (solid) films were used as a model system to study the effects of scaffold wall architecture on the differentiation of mouse ESC to osteoblastic lineage as a precursor to their use as a cell source for bone tissue engineering.

Materials and Methods

Materials

PLLA with an inherent viscosity of 1.6 dL/g was purchased from Alkermes (Medisorb; Cambridge, MA) and used without further purification. Dulbecco's modified Eagle's media (DMEM), 0.5 M EDTA, trypsin, Hank's buffered salt solution, and polymerase chain reaction (PCR) primers were obtained from Invitrogen (Carlsbad, CA). Fetal bovine serum (FBS) was obtained from Harlan Biological (Indianapolis, IN). Human recombinant leukemia inhibitory factor (LIF) and Neuronal Class III β-Tubulin (TUJ1) antibody were obtained from Chemicon (Temecula, CA).

Departments of [1]Biomedical Engineering, [2]Biologic and Materials Sciences, and [3]Macromolecular Science and Engineering Center, The University of Michigan, Ann Arbor, Michigan.

Brachyury antibody was obtained from Santa Cruz Biotechnology (Santa Cruz, CA). LEAF anti-mouse/rat CD49e, LEAF anti-mouse/rat CD49b, and LEAF Purified Armenian Hamster Immunoglobulin G (IGG) Isotype Control were obtained from Biolegend (San Diego, CA). All secondary antibodies and normal donkey serum were obtained from Jackson ImmunoResearch (West Grove, PA). RNeasy Mini Kit and Rnase-Free DNase set were obtained from Qiagen (Valencia, CA). TaqMan reverse transcription reagents, real-time PCR primers, and TaqMan Universal PCR Master Mix were obtained from Applied Biosystems (Foster City, CA). Chemicals were obtained from Sigma Chemical (St. Louis, MO) unless otherwise noted above.

Thin matrix preparation for cell culture

PLLA was dissolved in tetrahydrofuran at 60°C to make a 10% (w/v) PLLA solution. The NF PLLA matrix (thickness ~40 μm) was fabricated by first casting 0.4 mL of the PLLA solution on a glass support plate that had been preheated at 45°C for 10 min and then sealing the polymer solution on the glass support plate by covering it with another preheated glass plate. The polymer solution was phase separated at −20°C for 2 h and then immersed into a mixture of ice and water to exchange tetrahydrofuran for 24 h. The matrix was washed with distilled water at room temperature for 24 h with water changed every 8 h. The matrix was then freeze-dried. The porosity and fiber diameter were determined as previously described.[17] Briefly, the volume and the weight of the matrix were determined, and then the density was calculated. The porosity was then calculated from the measured overall densities. The average fiber diameter was calculated from scanning electron microscopy (SEM) micrographs. Fifty fibers per sample were measured, and their average and standard deviations are reported.

The matrices were cut to fit into a 35-mm Petri dish and secured in place with a disk of silicone elastomer from Dow Corning (Midland, MI) containing a 1.5 mm by 1.5 mm opening that had been cast from a 1:10 mix of curing agent to base. The matrices were then sterilized with ethylene oxide, wet with Hank's buffered salt solution two times for 0.5 h each, and rinsed with differentiation media (DMEM supplemented with 20% FBS, 10^{-4} M β-mercaptoethanol, and 1.33 μg/mL HEPES) for 1 h.

Solid films were fabricated in a similar manner excluding the phase separation step. Instead, the solvent was evaporated at room temperature in a fume hood. The flat films and 0.1% gelatin-coated Petri dishes were then treated similarly to the NF matrices.

Mouse ESC culture and seeding

D3 mouse ESC[22] were cultured on 0.1% gelatin-coated tissue culture flasks in ESC media (DMEM supplemented with 10% FBS, 10^{-4} M β-mercaptoethanol, 0.224 μg/mL L-glutamine, 1.33 μg/mL HEPES, and 1000 units/mL human recombinant LIF).

Fifteen thousand (for SEM to see the interactions of individual cells with the matrices) or 60,000 cells were seeded on each of the prepared matrices or 0.1% gelatin-coated tissue culture dish controls. Upon seeding, cells were cultured in differentiation media (DMEM supplemented with 20% FBS, 10^{-4} M β-mercaptoethanol, 0.224 μg/mL L-glutamine, and 1.33 μg/mL HEPES) or osteogenic media (differentiation media supplemented with 1 μM dexamethasone, 50 μg/mL ascorbic acid, and 10 mM β-glycerol phosphate). The media was changed 12 h after seeding and then every other day for the remainder of the culture period.

For the α2 integrin blocking studies, 6 μg/mL LEAF anti-mouse/rat CD49b antibody[23] was added to the media from day 7 onward, while for the α5 integrin blocking studies 6 μg/mL LEAF anti-mouse/rat CD49e antibody was added to the media after a 24 h attachment period.

Scanning electron microscopy

Twelve hours after seeding, the matrices and control were washed with phosphate-buffered saline (PBS) and 0.1 M cacodylate buffer, and then fixed with 2.5% glutaraldehyde in 0.1 M cacodylate buffer over night. The matrices were washed again with 0.1 M cacodylate buffer and postfixed in 1% osmium tetroxide for 1 h. The fixed samples were then dehydrated through an ethanol gradient (50%, 70%, 90%, 95%, and 100%) over 3 h and dried with hexamethyldisilazane. Samples were then gold coated and observed using SEM (S-3200; Hitachi, Tokyo, Japan). Cell spreading area was calculated from at least 20 cells per sample in the SEM images using the automated measure function of ImageJ (downloaded from the National Institutes of Health, Bethesda, MD; free download available at http://rsb.info.nih.gov/ij/).

Immunofluorescence and Alizarin Red S staining

For quantitative analysis, the ESC were removed from the matrices and 0.1% gelatin-coated tissue culture plastic control using 0.25% trypsin/1 mM EDTA. The cells were then fixed with 4% paraformaldehyde/0.2% triton-X100 in PBS, washed twice in 0.1% goat serum in PBS, and stained in 1 mg of Runx2 and TUJ1 antibodies in 100 mL of 0.2% Triton-X100/ 2% goat serum in PBS. The ESC were then washed twice with PBS and stained with the appropriate secondary antibodies and DAPI. The cells from each 12-day sample were then placed on a cover slip, and the number of ESC expressing Runx2 and TUJ1 were then counted in four random fields of view in each of three replicates. At least 900 cells as determined by DAPI staining in images taken with an RT Slider Spot Camera (Diagnostic Instraments, Sterling Heights, MI) on an Eclispe TE 300 fluorescence microscope (Nikon Instruments, Melville, NY) were counted per sample using Image-Pro Plus (Media Cybernetics, Bethesda, MD). Images of Runx2 and TUJ1 staining were overlaid with matching images of DAPI staining in Photoshop CS (Adobe, San Jose, CA). Areas of Runx2 and TUJ1 staining not associated with a nucleus were then manually excluded in Image-Pro Plus. All counts were checked with a counter by hand and found to be similar.

After 26 days of culture, the matrices and controls were fixed with 2% paraformaldehyde/PBS, washed, and stored at 4°C in PBS. Nonspecific antibody binding was blocked by incubating in 10% donkey or goat serum, and then the matrices and controls were exposed to TUJ1 (1:250) or osteocalcin (1:50) antibodies, followed by appropriate secondary antibodies conjugated to FITC (TUJ1), or TRITC (osteocalcin). DAPI was used to stain cell nuclei.

For Alizarin Red S staining, the matrices and controls were fixed using the same method as described above and then

stained with 40 mM Alizarin Red S solution, pH 4.2 at room temperature for 10 min. Matrices and controls were then rinsed five times in distilled water and washed three times in PBS on an orbital shaker at 40 rpm for 5 min each to reduce nonspecific binding.

Western blotting

Films were prewetted with PBS according to protocol described above, and then cell culture medium or 100 μg/mL bovine fibronectin was added and incubated for 1 h. For cell culture medium treatment, three films were pooled for sample collection, while one film was used to form fibronectin collection sample. Films were then washed with PBS for two times, cut into pieces, and transferred to 1.5 mL tubes. One milliliter of PBS was added, and the films were washed three times. PBS was then removed, and the films were centrifuged at 12,000 rpm for two times (1 min each) to remove remaining liquid. One hundred microliters of 1% sodium dodecyl sulphate was added and incubated for 1 h. This was repeated two more times, and the samples were pooled to form a 300 μL sample. Thirty microliters of the collection sample was used for each gel. Western blot analysis was conducted as previously described.[19] Briefly, the recovered serum protein samples were subject to fractionation through 4–12% sodium dodecyl sulphate–polyacrylamide gel electrophoresis. The fractionated proteins were transferred to a polyvinylidene fluoride (PVDF) membrane (Sigma). The blots were washed with Tris-Buffered Saline/TWEEN-20 (TBST) (10 mM Tris-HCl, 150 mM NaCl, and 0.05% Tween-20, pH 8.0), and blocked with Blotto (5% nonfat milk in TBST) at room temperature for 1 h. The blots were incubated in anti-bovine fibronectin polyclonal antibody (Santa Cruz Biotechnology) at room temperature for 1 h. After washing with TBST, the blots were incubated in anti-goat IGG-horseradish peroxidase–conjugated antibody (Sigma), and then in chemiluminescence reagent (SuperSignal West Dura; Pierce, Rockford, IL). The relative densities of the protein bands were analyzed with QualityOne (Biorad, Hercules, CA).

PCR and real-time PCR

Total RNA was isolated from at least three replicates using an RNeasy Mini Kit according to the manufacturer's protocol after films were mechanically homogenized with a Tissue-Tearor (BioSpec Products, Bartlesville, OK), while cells cultured on gelatin-coated tissue culture plate controls were harvested with a cell scraper. RNA samples with an optical density ratio of absorbance at 260 nm (RNA) over that at 280 nm (protein) greater than 1.6 were used to make cDNA. Based on the absorbance reading at 260 nm, 1 mg of RNA from each sample was used to make cDNA using a Geneamp PCR (Applied Biosystems) with TaqMan reverse transcription reagents. The thermocycler program was as follows: 10 min incubation at 25°C, 30 min reverse transcription at 48°C, and 5 min inactivation at 95°C. Five microliters of each reaction was subject to PCR using AmpliTaq Gold DNA polymerase (Applied Biosystems) for each of the following: brachyury (5′-gctgtgactgcctaccagcagaatg-3′ and 5′-gagagagagcgagcctccaaac-3′); nestin (5′-gtgcctctggatgatg-3′ and 5′-ttgaccttcctccccctc-3′); α5 integrin (5′-cgttgagtcattcgcctct-3′ and 5′-ctaccgcgtctaggttgaagc-3′); α2 integrin (5′-acccgccccttctgtatcttt-3′ and 5′-ggcagtcatagcca acagcaa-3′); β1 integrin (5′-ggtgtcgtgtttgtgaatgc-3′ and 5′-caca gttgtcacggcactct-3′); collagen type I (5′-gaagtcagctgcatacac-3′ and 5′-aggaagtccaggctgtcc-3′); Runx2 (5′-ccgcacgacaaccgcaccat-3′ and 5′-cgctccggcccacaaatctc-3′); bone sialoprotein (5′-gtca acggcaccagcaccaa-3′ and 5′-gtagctgtattcgtcctcat-3′); osteocalcin (5′-cggccctgagtctgacaaa-3′ and 5′-accttattgccctcctgcctt-3′); and β actin (5′-caggattccatacccaagaag-3′ and 5′-aaccctaaggccaaccgtg-3′). The cycling conditions were 94°C for 5 min followed by 94°C for 30 s, 55°C for 60 s, 72°C for 60 s 35 cycles for brachyury and β actin, 94°C for 120 s, 55°C for 30 s, 72°C for 45 s 35 cycles for nestin, 94°C for 60 s, 60°C for 120 s, 72°C for 180 s 40 cycles for α5 integrin, and 94°C for 30 s, 55°C for 60 s, 72°C for 60 s 30 cycles for α2 integrin, β1 integrin, Runx2, bone sialoprotein, and osteocalcin. These amplifications were followed by a 10 min extension at 72°C. The relative densities of the bands were analyzed with QualityOne (Biorad) to obtain a semi-quantitative assessment.

Real-time PCR was set up using TaqMan Universal PCR Master mix and specific primer sequence for brachyury, nestin, bone sialoprotein, osteocalcin, and β actin with 2 min incubation at 50°C, a 10 min Taq Activation at 95°C, and 50 cycles of denaturation for 15 s at 95°C, followed by an extension for 1 min at 72°C on an ABI Prism 7500 Real-Time PCR System (Applied Biosystems). Target genes were normalized against β actin using a relative standard curve.

Statistical analysis

All experiments were conducted at least three times. All quantifiable data are reported with the means and standard deviations. Student's *t*-tests were performed where applicable. Significance was set at $p \leq 0.05$.

Results

The surface characterization of the NF matrix (Fig. 1A) and the solid film (Fig. 1B) via SEM shows the differences in matrix architecture before cell culture. The NF matrix was found to contain fibers ranging in diameter from 50 to 500 nm with an average fiber diameter of 148 ± 21 nm (standard deviation) and calculated to have a porosity of 92.9%. The NF matrix contains very small pores preventing cellular penetration so that the effects of scaffold wall architecture can be studied without complications from cell distribution and mass transport conditions associated with pore size and inter-pore connectivity. Figure 1C illustrates the difference in cell morphology after 12 h of culture on NF PLLA matrix, solid PLLA film, and control surface (gelatin-coated tissue culture plastic). The differentiating ESC extended more processes on the NF matrix and spread to a greater degree ($278 \pm 56\ \mu m^2$ reported as area ± standard deviation) compared with ESC grown on either the solid film ($110 \pm 12\ \mu m^{2*}$, * indicates $p < 0.05$ compared to NF matrix) or control surface ($203 \pm 26\ \mu m^2$). Measurements of DNA content indicate that a similar number of cells have attached to each of the materials (data not shown), indicating that the cell morphology difference is not an effect of additional surface area available on the NF matrices.

Based on these initial morphological differences on the films, we examined cellular differentiation over longer culture periods. Brachyury mRNA expression (a mesodermal marker) and nestin (a neural marker) was examined in samples cultured in osteogenic media for 12 days (Fig. 2A). ESC cultured on the NF matrices were found to have increased brachyury

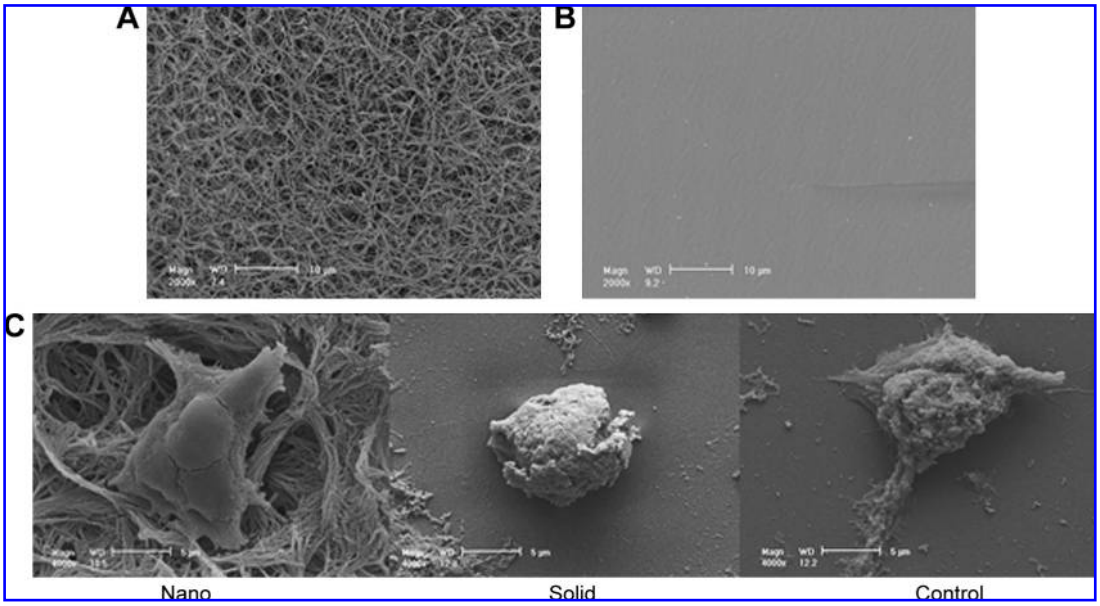

FIG. 1. SEM micrographs of (**A**) nanofibrous matrix, scale bar = 10 μm; (**B**) solid films, scale bar = 10 μm; and (**C**) D3 cells after 12 h under differentiation conditions on nanofibrous matrix (Nano), solid films (Solid), and gelatin-coated tissue culture plastic (Control), scale bar = 5 μm.

expression and reduced nestin expression compared to those on either the solid films or gelatin-coated control surface. Quantitative PCR results for brachyury expression (Fig. 2B) and nestin expression (Fig. 2C) show these relationships to be significant.

Early osteogenic markers (type I collagen and Runx2) were also examined via mRNA expression at day 12 (Fig. 2A). Type I collagen was found to be expressed more strongly in the ESC on the NF matrix and control then those on the solid films, while Runx2 was found to be expressed more strongly in the ESC on the NF matrix than either of those on the solid films or control. Later markers of bone differentiation, bone sialoprotein and osteocalcin, were not detectable at this time point.

Next, the percentage of cells on the matrices committed to the osteogenic lineage was examined after 12 days of osteogenic

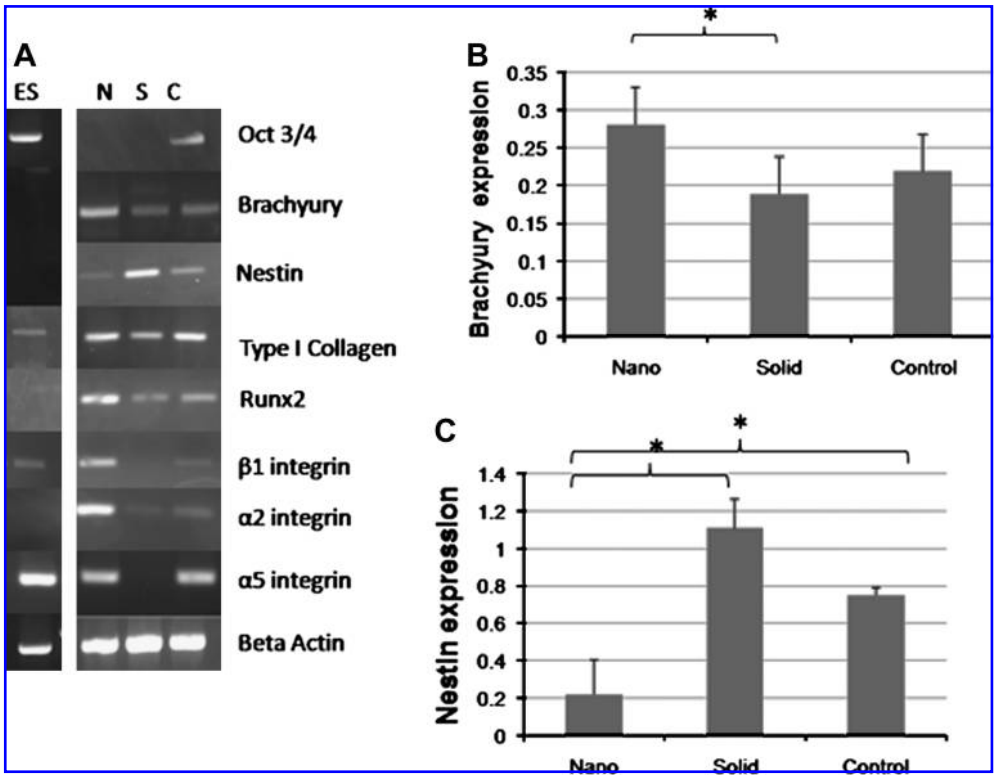

FIG. 2. Expression of neuronal, mesodermal, and early osteogenic markers and integrins after 12 days of culture under osteogenic conditions. (**A**) PCR on NF matrix (N), solid films (S), and gelatin-coated tissue culture plastic (C). (**B**) Quantification of brachyury expression on nanofibrous matrix (Nano), solid films (Solid), and gelatin-coated tissue culture plastic (Control); $^*p < 0.05$. (**C**) Quantification of nestin expression on nanofibrous matrix (Nano), solid films (Solid), and gelatin-coated tissue culture plastic (Control); $^*p < 0.05$.

culture. Approximately, $60 \pm 6\%$ (expression $\pm$ standard deviation) of ESC on the NF matrices expressed Runx2 at this time point, while only $33 \pm 11\%$ of ESC on the solid films and $38 \pm 2\%$ of ESC on the control. Expression of TUJ1, a neuronal marker, was also examined at this time. Approximately, $37 \pm 11\%$ (expression $\pm$ standard deviation) of ESC on the NF matrices expressed TUJ1, while $61 \pm 13\%$ of ESC on the solid films and $35 \pm 10\%$ of ESC on the control.

The expression of transcripts for several integrins ($\alpha 2$, $\alpha 5$, and $\beta 1$), cell membrane proteins that mediate cellular adhesion to substrates, were also examined after 12 days of culture in osteogenic media (Fig. 2A). Several integrin subunits associated with cellular adhesion to type I collagen ($\alpha 2\beta 1$) and fibronectin ($\alpha 5\beta 1$) were found to be upregulated on the NF matrices compared to the solid films. The increase in $\beta 1$ integrin transcription in ESC on NF matrices compared to solid films and control surface supports the lineage differentiation data, as increased $\beta 1$ integrin is associated with increased mesodermal differentiation while inhibiting neuronal differentiation.[24] Because integrin expression varies during osteogenesis as the ECM develops,[25] the ESC on the NF matrices may be changing their adhesion patterns and therefore gene expression as a response to more developed ECM being presented on the NF matrices than on either the solid films or the control surface.

To examine the effects of $\alpha 2$ and $\alpha 5$ integrins on the differentiation of ESC on the matrices, blocking studies were conducted (Fig. 3). Because $\alpha 2$ integrin expression is

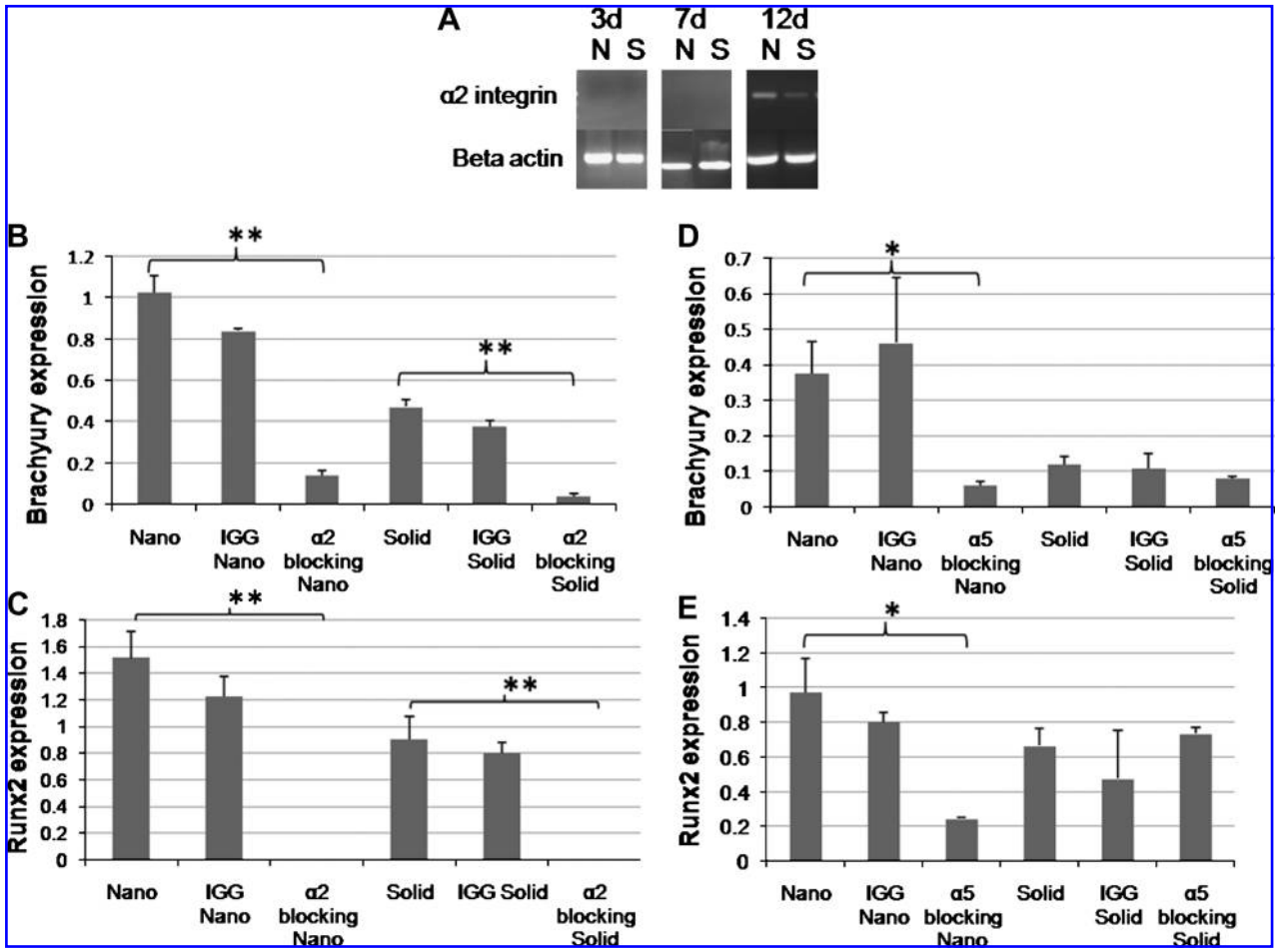

FIG. 3. Effects of integrin blocking on mesodermal and osteogenic differentiation after 12 days of differentiation culture. (**A**) PCR of $\alpha 2$ integrin RNA expression over time on nanofibrous matrix (N) and flat (solid) films (S). (**B**) Quantitative PCR of brachyury RNAs isolated from cells grown on nanofibrous matrix (Nano), on nanofibrous matrix with control IGG isotype (IGG nano), on nanofibrous matrix with CD49b antibody ($\alpha 2$ blocking nano), on flat (solid) films (Solid), on flat (solid) films with control IGG isotype (IGG solid), and on flat (solid) films with CD49b antibody ($\alpha 2$ blocking solid); $^{**}p < 0.01$. (**C**) Quantitative PCR of Runx2 RNAs isolated from cells grown on nanofibrous matrix (Nano), on nanofibrous matrix with control IGG isotype (IGG nano), on nanofibrous matrix with CD49b antibody ($\alpha 2$ blocking nano), on solid-walled matrix (Solid), on flat (solid) films with control IGG isotype (IGG solid), and on flat (solid) films with CD49b antibody ($\alpha 2$ blocking Solid); $^{**}p < 0.01$. (**D**) Quantitative PCR of brachyury RNAs isolated from cells grown on nanofibrous matrix (Nano), on nanofibrous matrix with control IGG isotype (IGG nano), on nanofibrous matrix with CD49e antibody ($\alpha 5$ blocking nano), on flat (solid) films (Solid), on flat (solid) films with control IGG isotype (IGG solid), and on solid-walled matrix with CD49e antibody ($\alpha 5$ blocking solid); $^{*}p < 0.05$. (**E**) Quantitative PCR of Runx2 RNAs isolated from cells grown on nanofibrous matrix (Nano), on nanofibrous matrix with control IGG isotype (IGG nano), on nanofibrous matrix with CD49e antibody ($\alpha 5$ blocking nano), on solid-walled matrix (Solid), on flat (solid) films with control IGG isotype (IGG solid), and on flat (solid) films with CD49e antibody ($\alpha 5$ blocking solid); $^{*}p < 0.05$.

developmentally regulated[26] and not expressed at the mRNA level in our undifferentiated cell population, a time course was conducted to determine when α2 integrin mRNA begins being transcribed during the differentiation process (Fig. 3A). Because this does not occur until after day 7 of differentiation, the blocking antibody was only administered to the cells from day 7 onward in the study. Figure 3B shows that blocking α2 integrin interactions substantially decrease mesodermal differentiation on both architectures. Runx2 was also examined after blocking α2 integrin, but after 70 amplification cycles no Runx2 expression was found in the samples treated with the α2 integrin blocking antibody, while the samples treated with the IGG isotype control antibody expressed Runx2 mRNA at a level similar to samples not exposed to antibodies (Fig. 3C). Measurements of DNA content indicate that a similar number of cells have attached to each of the NF matrices and solid film samples regardless of antibody treatment (data not shown), indicating that changes in cellular differentiation are not the result of variations in cell number present on the samples. Because α2 integrin interactions have been found to be necessary for the osteogenic differentiation of preosteoblasts, the lack of Runx2 mRNA expression, a characteristic of a more committed cell type,[23,27] in the samples where α2 integrin interactions were blocked was not surprising. Because α5 integrin is strongly expressed in our undifferentiated ESC,[28] blocking antibody was added to culture after a short attachment period to block its additional stimulation of differentiation signal transduction pathways such as focal adhesion kinase. Blocking α5 integrin interactions has a significant effect on both the mesodermal (Fig. 3D) and the osteogenic (Fig. 3E) differentiation of ESC cultured on the NF matrices but little effect on the mesodermal (Fig. 3D) and the osteogenic (Fig. 3E) differentiation of ESC cultured on the solid films. Because α5 integrin was downregulated at the mRNA level (Fig. 2A) on the solid films compared to the NF matrices and the effects of its stimulation on osteogenic differentiation have been shown to be dependent on culture conditions,[23,29] these results indicate that the NF matrices and the solid films expose the ESC grown on them to different microenvironments. One of the differences between the NF matrix and the solid film appears to be associated with α5 integrin interactions.

To examine the initial microenvironment created on each architecture, the protein adsorption from the differentiation media was examined (Fig. 4A). The NF matrices were found to adsorb more protein than the solid films. Western blots for fibronectin on NF matrices exposed to differentiation media (Fig. 4B) or pure bovine fibronectin (Fig. 4C) were shown to

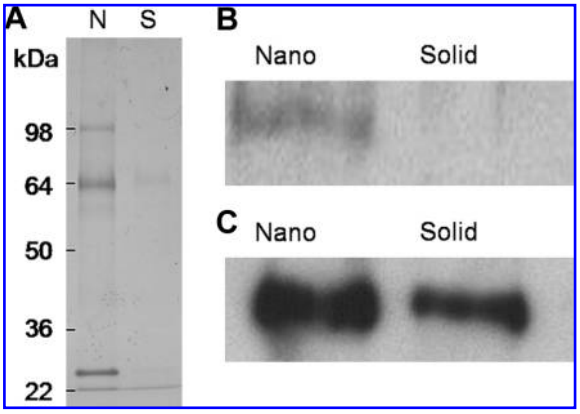

FIG. 4. Protein adsorption to materials after exposure to differentiation media containing 20% bovine serum protein or purified bovine fibronectin (100 μg/mL) for 1 h: (**A**) 4–12% polyacrylamide gels stained with Coomassie blue from protein extracts from nanofibrous matrix (N) and flat (solid) films (S) treated with media; (**B**) Western blot of fibronectin extracted from nanofibrous matrix (Nano) and flat (solid) films (Solid) treated with media; (**C**) Western blot of fibronectin extracted from nanofibrous matrix (Nano) and flat (solid) films (Solid) treated with purified bovine fibronectin.

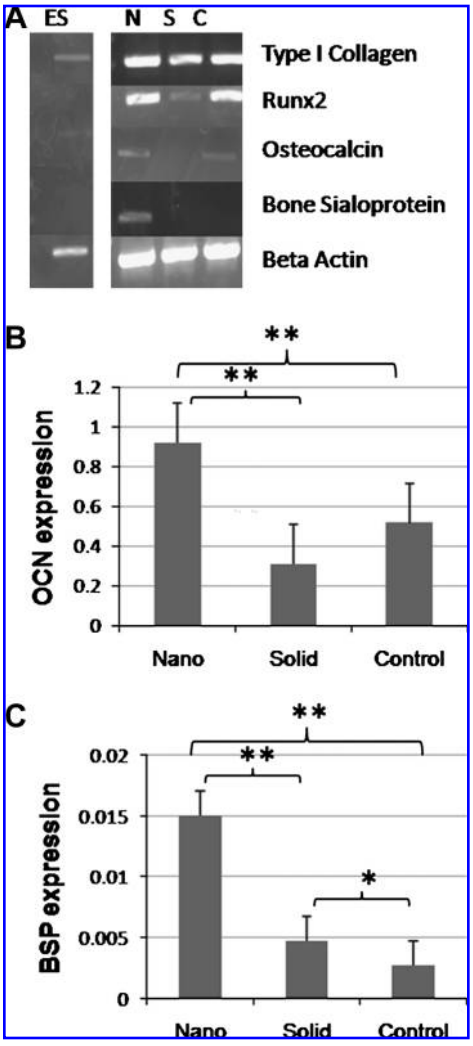

FIG. 5. Expression of osteogenic markers after 26 days of culture under osteogenic differentiation conditions. (**A**) PCR of RNAs isolated from cells grown on nanofibrous matrix (N), flat (solid) films (S), and gelatin-coated tissue culture plastic (C). (**B**) Quantitative PCR of osteocalcin RNAs isolated from cells grown on nanofibrous matrix (Nano), flat (solid) films (Solid), and gelatin-coated tissue culture plastic (Control); $^{**}p < 0.01$. (**C**) Quantitative PCR of bone sialoprotein RNAs isolated from cells grown on nanofibrous matrix (Nano), flat (solid) films (Solid), and gelatin-coated tissue culture plastic (Control); $^{*}p < 0.05$ and $^{**}p < 0.01$.

adsorb more fibronectin than similarly treated solid films, supporting the α5 integrin blocking data.

The expression of bone markers was examined after 26 days of differentiation (Fig. 5A). Type I collagen, unlike 12 days of differentiation, was expressed at a similar level on all materials and controls. While after the additional culture time, Runx2 was more strongly expressed on all materials and controls, it was still expressed more strongly on NF matrices than on solid films. Later markers of osteogenic differentiation (bone sialoprotein and osteocalcin) were now detected unlike the earlier time point. ESC grown on the NF matrices expressed higher levels of osteocalcin (Fig. 5B) and bone sialoprotein (Fig. 5C) compared to both solid films (3 times for both markers) and control surfaces (1.8 and 5.5 times, respectively).

The expression of these late-stage bone markers coincides with the mineralization of the matrix during bone formation. After 26 days of osteogenic culture, the samples were stained for calcium to examine mineral deposition on each of the surfaces (Fig. 6A). Although all the samples showed some degree of calcium deposition, there was substantially more calcium on the NF matrices than on the solid films or the controls. NF matrix without cells cultured in media for the same time period did not show significant staining (Fig. 6B), signifying that the mineralization on the NF matrices is due to cellular deposition and not biomimetic absorption from the media. Immunohistochemical localization of osteocalcin and TUJ1 was used to determine the distribution of the mature osteoblasts across the matrices (Fig. 6C). NF matrices had an even distribution of osteocalcin across the surface with very little neuronal differentiation, while solid films and controls had less osteocalcin protein and increased neuronal differentiation. NF matrix controls either without cells or without antibodies indicate that the staining is specific for osteocalcin and TUJ1 and not nonspecific binding of the antibody to the NF matrix. In combination with the

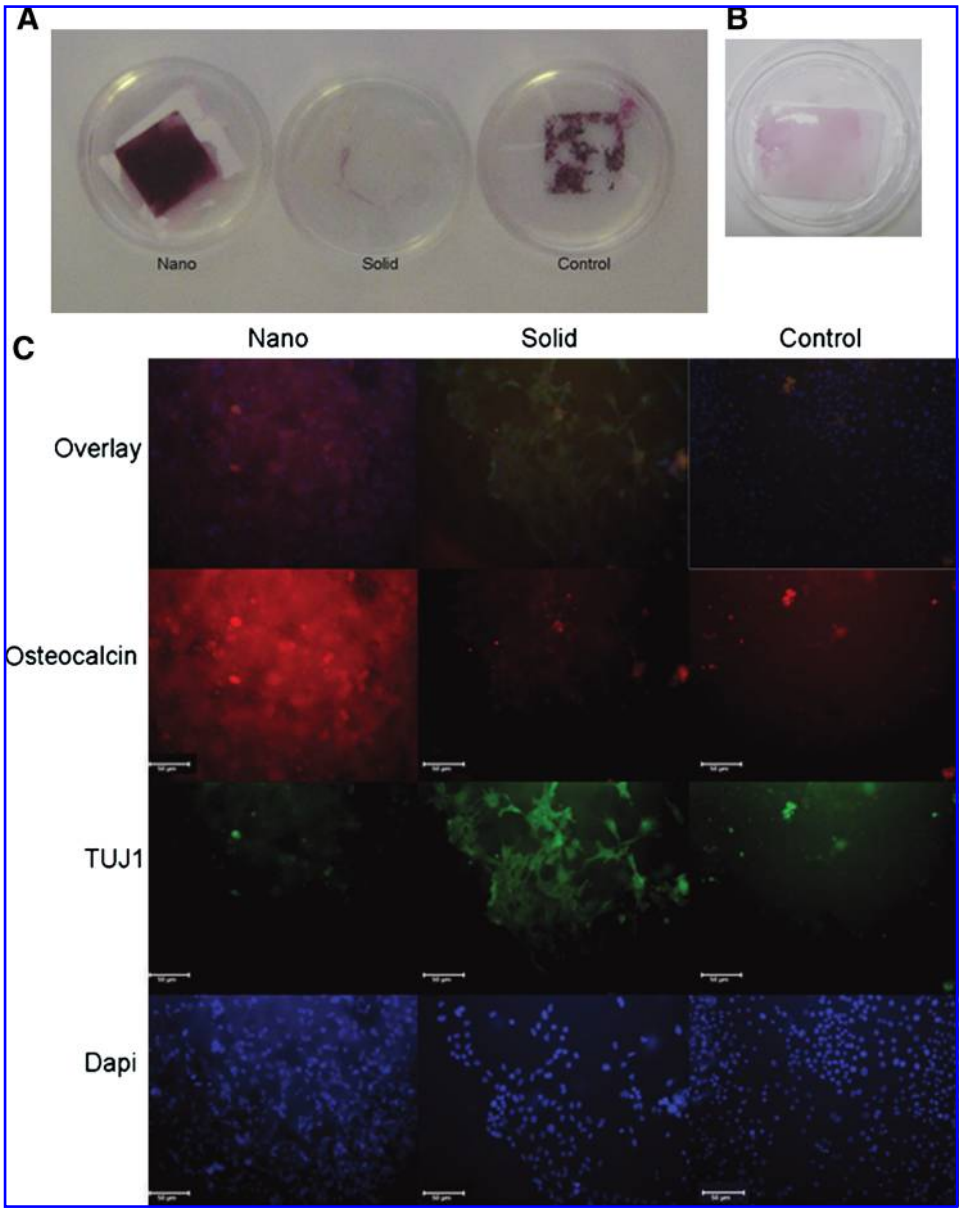

FIG. 6. Mineralization and extracellular characterization after 26 days of culture under osteogenic differentiation conditions. (**A**) Calcium staining after 26 days under osteogenic differentiation conditions on nanofibrous matrix (Nano), solid films (Solid), and gelatin-coated tissue culture plastic (Control). (**B**) Calcium staining after 26 days under osteogenic differentiation conditions on nanofibrous matrix without ESC. (**C**) Immunofluorescence localization neuronal (TUJ1) and late bone differentiation (Osteocalcin) marker expression after 26 days under osteogenic differentiation conditions on nanofibrous matrix (Nano), solid films (Solid), and gelatin-coated tissue culture plastic (Control). Scale bar = 50 μm. Color images available online at www.liebertonline.com/ten.

mRNA and mineralization data, this indicates that a more mature osteogenic cell population has differentiated on the NF matrix than on either the solid films or the control surface, suggesting that the NF matrix promotes greater differentiation of ESC toward the osteogenic lineage than the solid films or control surface.

Discussion

The controlled differentiation of ESC is a necessary first step in using them as a cell source for tissue engineering applications.[30] Current attempts focus on the use of biochemical factors to direct the differentiation of the cells to a particular lineage. However, biochemical cues are only part of the complex environment, which controls lineage fate *in vivo*. To elicit more control over lineage fate, one must move beyond chemical cues and examine how other components contribute. In this study, we have examined the effects of NF architecture on ESC differentiation using thin PLLA NF matrices as a model for tissue engineering applications.

With osteoblasts and their precursors, it has been shown that substrate architecture independent of material chemistry can significantly affect cellular behavior.[31–33] Osteoblasts in short-term culture on materials with NF architecture have been shown to extend more processes than osteoblasts cultured on material with solid architecture.[34] This is consistent with the enhanced ESC spreading and process outgrowth observed after 12 h on NF matrices compared to solid films. This is significant because the solid films were made of the same polymer, indicating that the NF architecture was contributing to the difference in cellular response and not the polymer itself. The increased cell spreading and process outgrowth with the NF matrices compared to the solid films may lead to increased activation of signaling pathways affecting lineage fate and the type of tissue formed.

As culture time increased, ESC on NF matrices with osteogenic supplementation continued to exhibit increased differentiation toward bone compared to ESC on the solid films. Increased differentiation on NF architecture compared to solid architecture has also been observed with osteoblasts.[20,34] In addition to the size scale of the material architecture, increased matrix rigidity have been reported to increased osteogenic differentiation of preosteoblastic cells.[32–34]

Several factors likely contribute to the differences in differentiation observed between the NF matrices and the solid films. Similar to the thin matrices and films (Fig. 4), previous work with macroporous NF PLLA scaffolds formed by a similar phase separation process showed that NF scaffolds adsorbed more serum proteins than solid-walled scaffolds and that the profile of the adsorbed proteins was different from those adsorbed by the solid-walled scaffolds.[19] Differences in the amount or type of adsorbed serum proteins may provide a better niche for directing the differentiation of ESC. Previously, we reported that similar NF scaffolds adsorb nearly four times more fibronectin than their solid counterparts.[19] Increased fibronectin adsorbed to the NF matrices may accelerate ESC differentiation to the mesodermal and osteogenic lineages on the NF matrices compared to the solid films, which is further supported by our α5 blocking results. Increased integrin signaling and differentiation have been observed in ESC cultured on fibronectin.[28] Fibronectin is the earliest of the matrix proteins synthesized by osteoblasts.[35,36] During embryonic development, integrin–fibronectin interactions have been shown to be important to early mesodermal development.[37]

A previous study found increased β1 integrin expression and osteogenic differentiation in neonatal mouse osteoblasts on NF scaffolds compared to their solid counterparts.[34] β1 Integrin expression is upregulated in a similar manner on the thin NF matrices compared to the solid films, which is consistent with the increased osteogenic differentiation and consistent with the observation that β1 integrin plays a role in mesodermal lineage commitment of ESC.[24] As such, increased stimulation of β1 integrin, which has been shown to regulate ESC differentiation through the MAP kinase signaling pathway,[38,39] could also be contributing to this increased ESC differentiation on the NF matrices compared to the solid films.

The NF matrices themselves mimic the fiber diameter of type I collagen, a major component of the bone ECM.[27] α2β1 Integrin is the major type I collagen binding integrin.[40,41] Although α2 integrin expression is developmentally regulated,[26] its upregulation has been linked to a increase in ESC differentiation[28] and is necessary for osteogenic differentiation[23,27] as seen in our α2 integrin blocking data (Fig. 3). A study of neonatal mouse osteoblasts on NF scaffolds indicates that α2β1 integrin could directly interact with the nanofibers based on their unaltered expression when collagen fiber formation was blocked.[34] Additionally, preosteoblasts were found to have unaltered cytoskeleton structure (in terms of stress fiber and focal adhesion formation) on gelatin-modified and -unmodified NF matrices.[42] As both eliminating the cell-produced collagen fibers and providing a collagen-like surface chemistry on the NF matrices did not eliminate or induce the NF effect, the NF architecture itself could be influencing cell behavior directly in a manner similar to type I collagen.

Conclusions

These results indicate that NF architecture contributes to promoting the osteogenic lineage fate of ESC cells. We observed morphological differences in ESC cultured on NF matrices compared to solid films in short time frames and increased differentiation to the mesodermal and osteogenic lineage (osteogenic media) over longer time frames. Based on these results, we believe that NF architecture plays an important role in differentiation and should be used in combination with soluble factors to achieve the directed differentiation necessary for tissue engineering applications.

Acknowledgments

The authors would like to thank Dr. K. Sue O'Shea for her gift of the D3 cells, Dr. Renny Franceschi for critical discussions, and Tianhan Wang and Erin Gatenby for their technical assistance. This research was partially supported by Michigan Center for hES Cell Research (NIH P20GM069985, Pilot PI: P.X.M.), NSF Graduate Student Fellowship (L.A.S.), and the NIH (NIDCR DE017689 and DE015384: P.X.M.).

Disclosure Statement

No competing financial interests exist.

References

1. Martin, G.R. Isolation of a pluripotent cell line from early mouse embryos cultured in medium conditioned by teratocarcinoma stem cells. Proc Natl Acad Sci USA **78,** 7634, 1981.
2. Evans, M.J., and Kaufman, M.H. Establishment in culture of pluripotential cells from mouse embryos. Nature **292,** 154, 1981.
3. Guillot, P.V., Cui, W., Fisk, N.M., and Polak, D.J. Stem cell differentiation and expansion for clinical applications of tissue engineering. J Cell Mol Med **11,** 935, 2007.
4. McCloskey, K., Gilroy, M., and Nerem, R. Use of embryonic stem cell-derived endothelial cells as a cell source to generate vessel structures *in vitro*. Tissue Eng **11,** 497, 2005.
5. Ke, Q., Yang, Y., Rana, J., Yu, C., Morgan, J., and Yong-Fu, X. Embryonic stem cells cultured in biodegradable scaffold repair infarcted myocardium in mice. Acta Physiologica Sinica **57,** 673, 2005.
6. Chaudhry, G., Yao, D., Smith, A., and Hussain, A. Osteogenic cells derived from embryonic stem cells produced bone nodules in three-dimensional scaffolds. J Biomed Biotechnol **4,** 203, 2004.
7. Randle, W.L., Cha, J.M., Hwang, Y.S., Chan, K.L., Kazarian, S.G., Polak, J.M., and Mantalaris, A. Integrated 3-dimensional expansion and osteogenic differentiation of murine embryonic stem cells. Tissue Eng **13,** 2957, 2007.
8. Buttery, L., Bourne, S., Xynos, J.D., Wood, H., Hughes, F.J., Hughes, S.P.F., Episkopou, V., and Polak, J.M. Differentiation of osteoblasts and *in vitro* bone formation of murine embryonic stem cells. Tissue Eng **7,** 89, 2001.
9. Kramer, J., Bohrnsen, F., Schlenke, P., and Rohwedel, J. Stem cell-derived chondrocytes for regenerative medicine. Transplant Proc **38,** 762, 2006.
10. Lavon, N., and Benvenisty, N. Study of hepatocyte differentiation using embryonic stem cells. J Cell Biochem **96,** 1193, 2005.
11. Hall, B., and Miyake, T. Divide, accumulate, differentiate: cell condensation in skeletal development revisited. Int J Dev Biol **39,** 881, 1995.
12. MacDonald, M., and Hall, B. Altered timing of the extracellular-matrix-mediated epithelial-mesenchymal interaction that initiates mandibular skeletogenesis in three inbread strains of mice: development, heterchrony and evolutionary change in morphology. J Exp Zool **291,** 258, 2001.
13. Aszodi, A., Bateman, J.F., Gustafsson, E., Boot-Handford, R., and Fassler, R. Mammalian skeletogenesis and extracellular matrix: what can we learn from knockout mice? Cell Struct Funct **25,** 73, 2000.
14. Ma, P.X. Biomimetic materials for tissue engineering. Adv Drug Delivery Rev **60,** 184, 2008.
15. Elsdale, T., and Bard, J. Collagen substrata for studies on cell behavior. J Cell Biol **54,** 626, 1972.
16. Birk, D.E., Silver, F.H., and Trelstad, R.L. Matrix assembly. In: Hay, E.D, ed. Cell Biology of the Extracellular Matrix. New York: Plenum Press, 1991.
17. Ma, P.X., and Zhang, R. Synthetic nano-scale fibrous extracellular matrix. J Biomed Mater Res **46,** 60, 1999.
18. Chen, V., and Ma, P.X. Nano-fibrous poly(L-lactic acid) scaffolds with interconnected spherical macropores. Biomaterials **25,** 2065, 2004.
19. Woo, K.M., Chen, V.J., and Ma, P.X. Nano-fibrous scaffolding architecture selectively enhances protein adsorption contributing to cell attachment. J Biomed Mater Res **67A,** 531, 2003.
20. Chen, V., Smith, L., and Ma, P.X. Bone regeneration on computer-designed nano-fibrous scaffolds. Biomaterials **27,** 3973, 2006.
21. Zhang, R., and Ma, P.X. Synthetic nano-fibrillar extracellular matrices with predesigned macroporous architectures. J Biomed Mater Res **52,** 430, 2000.
22. Doetschman, T., Eistetter, H., Katz, M., Schmidt, W., and Kemler, R. The *in vitro* development of blastocyst-derived embryonic stem cell lines: formation of visceral yolk sac, blood island and myocardium. J Embryol Exp Mophol **87,** 27, 1985.
23. Xiao, G., Wang, D., Benson, D., Karsenty, G., and Franceschi, R.T. Role of the a2-integrin osteoblast-specific gene expression and activation of the OSF2 transcription factor. J Biol Chem **273,** 32988, 1998.
24. Rohwedel, J., Guan, K., and Zuschratter, W. Loss of beta 1 integrin function results in a retardation of myogenic, but an acceleration of neuronal, differentiation of embryonic stem cells *in vitro*. Del Biol **201,** 167, 1998.
25. Siebers, M., ter Brugge, P., Walboomers, X., and Jansen, J. Integrins as a linker protein between osteoblasts and bone replacing materials. A critical review. Biomaterials **26,** 137, 2005.
26. Sutherland, A.E., Calarco, P.G., Damsky CH. Developmental regulation of integrin expression at the time of implantation in the mouse embryo. Development **119,** 1175, 1993.
27. Mizuno, M., Fujisawa, R., and Kuboki, Y. Type I collagen-induced osteoblastic differentiation of bone-marrow cells mediated by collagen-alpha2beta1 integrin interaction. J Cell Physiol **184,** 207, 2000.
28. Hayashi, Y., Furue, M.K., Okamoto, T., Myoishi, Y., Fukuhara, Y., Abe, T., Sato, J.D., Hata, R.I., and Asashima, M. Integrins regulate mouse embryonic stem cell self-renewal. Stem Cells **25,** 3005, 2007.
29. Jikko, A., Harris, S.E., Chen, D., Mendrick, D.L., and Damsky, C.H. Collagen integrin receptors regulate early osteoblast differentiation induced by BMP-2. J Bone Miner Res **14,** 1075, 1999.
30. Vats, A., Tolley, N., Bishop, A., and Polak, J. Embryonic stem cells and tissue engineering: delivering stem cells to the clinic. J R Soc Med **98,** 346, 2005.
31. Fleming, R., Murphy, C., Abrams, G., Goodman, S., and Nealey, P. Effects of synthetic micro-and nano-structured surfaces on cell behavior. Biomaterials **20,** 573, 1999.
32. Keselowsky, B.G., Wang, L., Schwartz, Z., Garcia, A.J., and Boyan, B.D. Integrin alpha(5) controls osteoblastic proliferation and differentiation responses to titanium substrates presenting different roughness characteristics in a roughness independent manner. J Biomed Mater Res A **80,** 700, 2007.
33. Lim, J.Y., Hansen, J.C., Siedlecki, C.A., Runt, J., and Donahue, H.J. Human foetal osteoblastic cell response to polymer-demixed nanotopographic interfaces. J R Soc Interface **22,** 97, 2005.
34. Woo, K.M., Jun, J.-H., Chen, V.J., Seo, J., Baek, J.-H., Ryoo, H.-M., Kim, G.-S., Somerman, M.J., and Ma, P.X. Nano-fibrous scaffolding promotes osteoblast differentiation and biomineralization. Biomaterials **28,** 335, 2007.
35. Weiss, R., and Reddi, A. Role of fibronectin in collagenous matrix-induced mesenchymal cell proliferation and differentiation *in vivo*. Exp Cell Res **133,** 247, 1981.
36. Cowles, E., DeRome, M., Pastizzo, G., Brailey, L., and Gronowicz, G. Mineralization and the expression of the matrix proteins during *in vivo* bone development. Calcif Tissue Int **62,** 74, 1998.

37. Yang, J.T., Bader, B.L., Kredberg, J.A., Ullman-Cullere, M., Trevithick, J., and Hynes, R.O. Overlapping and independent functions of fibronectin receptor integrins in early mesodermal development. Dev Biol **215,** 264, 1999.
38. Watt, F., and Hogan, B. Out of Eden: stem cells and their niches. Science **287,** 1427, 2000.
39. Czyz, J., and Wobus, A. Embryonic stem cell differentiation: the role of extracellular factors. Differentiation **68,** 167, 2001.
40. Tulla, M., Pentikainen, O.T., Viitasalo, T., Kapyla, J., Impola, U., Nykvist, P., Nissinen, L., Johnson, M.S., and Heino, J. Selective binding of collagen subtypes by integrin alpha 1I, alpha 2I, and alpha 10I domains. J Biol Chem **276,** 48206, 2001.
41. Kapyla, J., Ivaska, J., Riikonen, R., Nykvist, P., Pentikainen, O., Johnson, M.S., and Heino, J. Integrin alpha(2)I domain recognizes type I and type IV collagens by different mechanisms. J Biol Chem **275,** 3348, 2000.
42. Hu, J., Liu, X., and Ma, P.X. Induction of osteoblast differentiation phenotype on poly(L-lactic acid) nanofibrous matrix. Biomaterials **29,** 3815, 2008.

Address correspondence to:
Peter X. Ma, Ph.D.
Department of Biologic and Material Sciences
The University of Michigan
Room 2211, 1011 North University Ave.
Ann Arbor, MI 48109-1078

E-mail: mapx@umich.edu

Received: April 17, 2008
Accepted: November 13, 2008
Online Publication Date: January 5, 2009

This article has been cited by:

1. Yash M. Kolambkar , Alexandra Peister , Andrew K. Ekaputra , Dietmar W. Hutmacher , Robert E. Guldberg . 2010. Colonization and Osteogenic Differentiation of Different Stem Cell Sources on Electrospun Nanofiber MeshesColonization and Osteogenic Differentiation of Different Stem Cell Sources on Electrospun Nanofiber Meshes. *Tissue Engineering Part A* **16**:10, 3219-3230. [Abstract] [Full Text] [PDF] [PDF Plus]
2. Seth D. McCullen , Philip R. Miller , Shaun D. Gittard , Russell E. Gorga , Behnam Pourdeyhimi , Roger J. Narayan , Elizabeth G. Loboa . 2010. In Situ Collagen Polymerization of Layered Cell-Seeded Electrospun Scaffolds for Bone Tissue Engineering ApplicationsIn Situ Collagen Polymerization of Layered Cell-Seeded Electrospun Scaffolds for Bone Tissue Engineering Applications. *Tissue Engineering Part C: Methods* **16**:5, 1095-1105. [Abstract] [Full Text] [PDF] [PDF Plus]
3. Seth D. McCullen , Jackie Zhan , Maureen L. Onorato , Susan H. Bernacki , Elizabeth G. Loboa . 2010. Effect of Varied Ionic Calcium on Human Adipose-Derived Stem Cell MineralizationEffect of Varied Ionic Calcium on Human Adipose-Derived Stem Cell Mineralization. *Tissue Engineering Part A* **16**:6, 1971-1981. [Abstract] [Full Text] [PDF] [PDF Plus]
4. Ian O Smith, Peter X Ma. 2010. Cell and biomolecule delivery for regenerative medicine. *Science and Technology of Advanced Materials* **11**:1, 014102. [CrossRef]
5. Seth D. McCullen, Carla M. Haslauer, Elizabeth G. Loboa. 2010. Fiber-reinforced scaffolds for tissue engineering and regenerative medicine: use of traditional textile substrates to nanofibrous arrays. *Journal of Materials Chemistry* **20**:40, 8776. [CrossRef]